

## Development of Ductile Engineered Cementitious Composite Elements for Seismic Structural Applications

V.C. Li<sup>1</sup>, H. Fukuyama<sup>2</sup>, and A. Mikame<sup>3</sup>

<sup>1</sup>ACE-MRL, Department of Civil and Environmental Engineering,  
University of Michigan, Ann Arbor, MI 48109-2125 USA

<sup>2</sup>International Institute of Seismology and Earthquake Engineering  
Building Research Institute, Japanese Ministry of Construction, Tsukuba, Japan

<sup>3</sup>Technical Research Institute, Fujita Corporation, Yokohoma, Japan

### INTRODUCTION

A collaborative effort between US and Japanese researchers since 1996 has focused on the development of ductile critical elements for various structural applications, based on a new materials technology. The new materials technology involves an Engineered Cementitious Composite (ECC) microstructurally designed using micromechanical principles. ECC exhibits strain-hardening in tension with strain-capacity in excess of 4%. The ultra ductile behavior of ECC, combined with its flexible processing requirements, isotropic properties, and moderate fiber content (typically < 2% depending on fiber type and interface and matrix characteristics) make it especially suitable for critical elements in seismic applications where high performance such as energy absorption, steel/concrete deformation compatibility, and spall resistance are required. Applications to both new structures and in retrofitting of existing R/C structures to withstand future earthquakes are considered.

### DEVELOPMENT OF ECC MATERIALS

The development of ECC is based on the micromechanics of fiber bridging and matrix crack extension. The theoretical foundation was first described by Li (1993) and further detailed in Li et al (1996) and Li (1997). As a result of the micromechanics analyses, it was shown that pseudo strain-hardening under tensile loading can be accomplished with short randomly oriented fiber reinforcement of a cementitious matrix, at moderate dosage no more than 2% by volume. Various fiber types can be utilized as long as the fiber volume fraction  $V_f$  satisfies:

$$V_f > V_f^{crit} \equiv \frac{12J_c}{g\tau(L_f/d_f)\delta_o} \quad (1)$$

where  $\delta_o = \tau L_f^2 / [E_f d_f (1 + \eta)]$  is the crack opening corresponding to the maximum bridging stress. Also  $\eta = (V_f E_f) / (V_m E_m)$ , where  $V_m$  and  $E_m$  are the matrix volume fraction and Young's Modulus, respectively. Supplementary conditions are described in Li and Leung (1992). The critical fiber volume fraction  $V_f^{crit}$  is therefore dependent on fiber, matrix and fiber/matrix interaction properties. Fiber properties include fiber length  $L_f$ , diameter  $d_f$ , and modulus  $E_f$ . The fiber/matrix interaction properties include friction  $\tau$  and a snubbing factor  $g$  (Li et al, 1990). The matrix properties include matrix modulus  $E_m$  and matrix toughness  $J_c$ .

It should be noted that Eq. (1) is applicable only to the case when fiber rupture does not occur, and that the fiber/matrix interface is governed only by simple friction with no chemical bond. Extension of (1) to composites with these properties have been considered by Maalej et al (1995), Kanda and Li (1997). The reformulation of (1) leads to  $V_f^{crit}$  which depends on fiber strength  $\sigma_f$  and chemical bond strength  $\tau_c$ , in addition to those already mentioned above.

Equation (1) prescribes the recipe for formulating a ECC material systematically. It guides the composite design by specifying the necessary combinations of fiber, matrix and fiber/matrix interaction properties. Most current FRCs would have these micromechanical parameter combinations which lead to high  $V_f^{crit}$ . This means that unless the fiber volume fraction is high, (say e.g.  $> V_f^{crit} = 10\%$ ), pseudo strain hardening cannot be achieved. The power of Eqn. (1) is to allow systematic tailoring of the micromechanical properties in order to

achieve a low to moderate  $V_f^{crit}$ . For example, fiber diameter typically ranges from 10 micron to 500 micron, bond properties vary from much less than 1 MPa to 10 MPa, and matrix toughness can range from 0.001 kJ/m<sup>2</sup> to .1 kJ/m<sup>2</sup>. The ACE-MRL has demonstrated pseudo strain hardening properties with ECCs reinforced with PE and PVA fibers with volume fraction less than or equal to 2%.

Some mechanical properties of these two ECCs are summarized below. Details can be found in Li (1997) and Kanda and Li (1997). Due to space limitation, only tensile, compressive, shear, and damage tolerant properties are further discussed here. For some tests, both monotonic and fully reversed cyclic load sequence are applied. A summary of these properties can be found in Table 1. The material database serves as the starting point of the construction of new constitutive models which are used together with finite element techniques to evaluate the potential performance of ECC structural elements. Some results of such evaluations are included in the following Section to indicate the transfer of ECC material properties to ECC structural element response.

TABLE 1: Properties of ECC

	Tensile				Compressive		Stiffness	Flexural	Fracture
	$\sigma_{fc}$ (MPa)	$\epsilon_{fc}$ %	$\sigma_{cu}$ (MPa)	$\epsilon_{cu}$ %	$f'_c$ (MPa)	$\epsilon'_c$ %	E (GPa)	MOR (MPa)	J (kJ/m <sup>2</sup> )
PE-ECC	2.5	0.021	4.6	5.6	68.5	0.67	22	12.5	27
PVA-ECC	2.2	-	3.1	1.5	35	0.45	16	-	-

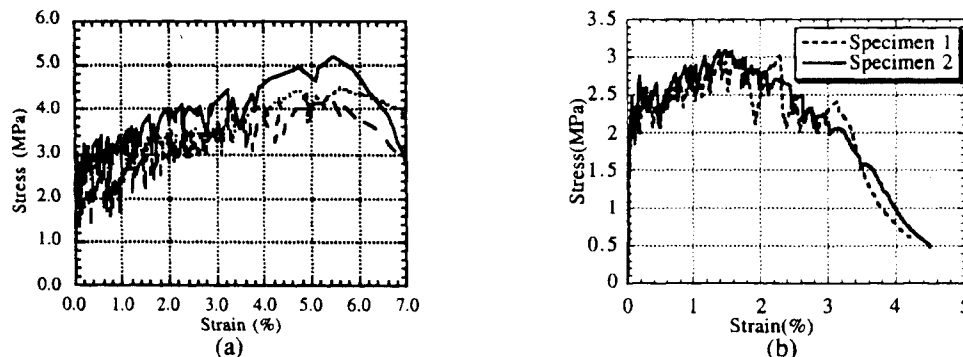


Fig. 1: Stress-Strain Curves Measured for (a) PE-ECC; and (b) PVA-ECC

### Uniaxial Tension

Figure 1a shows a typical tensile stress-strain curve of a PE-ECC. The ECC shows a clear pseudo-strain hardening behavior with an average strain at peak stress  $\epsilon_{cu}$  approximately equal to 5.6 % (about 560 time the strain capacity of the unreinforced matrix). After first cracking, the load continues to rise with no fracture localization. For this composite, real-time observation showed that multiple cracking occurred with many sub-parallel cracks across the specimen during strain-hardening. Beyond peak stress, localized crack opening occurred accompanied by fiber bridging. All fibers are pulled out in this ECC. Also shown in Figure 1b is the tensile stress-strain curve of a PVA-ECC (Kanda and Li, 1997). Uniaxial tensile-compression cyclic behavior of ECC is currently being investigated in Japan.

### Uniaxial Compression

The cylinder compressive strength of a PE-ECC is approximately 68 MPa. The compressive strain capacity has been observed to increase by approximately 40% over normal concrete and FRCs. The corresponding compressive strength for a PVA-ECC is about 35 MPa. The matrix mix design for the PVA-ECC has been modified to take into account the different bridging property of the PVA fiber in comparison to the PE fiber.

### Shear

Figure 2 shows shear response of a PE-ECC, conducted under a pure-shear panel set-up at Tsukuba University. Many sub-parallel microcracks were observed during loading, and the maximum shear strain

reached around 1.8%, almost the same level as steel reinforced mortar panels. The final failure was accompanied by six visible cracks with fiber pull-out in the mid-diagonal opening crack. Compressive failure of cracked mortar was not observed. The same test conducted using FRC panels revealed brittle failure with a single diagonal crack. These findings are consistent with those of an investigation on shear response of an PE-ECC using Ohno Shear beams (Li et al. 1994). A 2.6% failure strain was observed in that experiment.

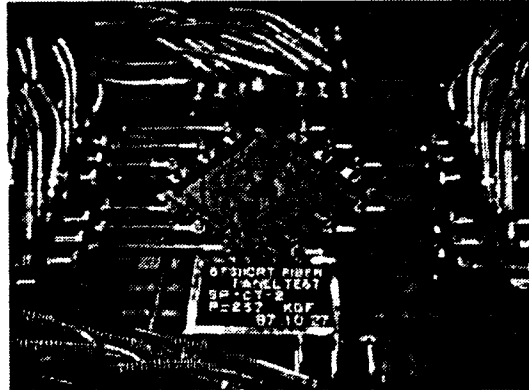


Fig. 2: Pure Shear Test Showing Failure Mode of PE-ECC

### *Damage Tolerance*

Notched specimens of PE-ECC are tested for damage tolerance (Li, 1997). The tensile load deformation curves of these plates (Fig. 3) show extensive inelastic straining for both notched and unnotched specimens. Specimen width is 76mm. U-3 and U-7 have notch lengths of 15 mm, while U-4 and U-8 have notch lengths of 20 mm. U-28 is unnotched. The peak load is plotted as a function of the reduced section of the notched specimens in Fig. 4 which also shows the linear reduction line for constant strength. The data of the notched specimen lying near (and actually slightly above) this line suggests that these composites are notch-insensitive. The surface of the notched specimen (Fig. 5) shows multiple cracks typical of strain hardening fiber reinforced composites. Although the ultimate localized fracture is in the reduced section, multiple cracking spreads along the full length of the specimens prior to final failure.

## PERFORMANCE OF ECC STRUCTURAL ELEMENTS

Mechanical tests of ECC structural elements to confirm the expected performance and to provide feedback for further material refinements have been conducted. As well, the structural element response obtained will be used to guide structural system tests and dynamic analyses of system response under representative seismic load spectrums. The ultimate goal of this effort is to develop design guidelines for practical structural systems containing ECC elements (Fig. 6)

ECCs can be adopted in energy absorption devices such as wall members, and in structural elements under high stresses such as short span beam and column end for RC structures designed for new construction and seismic retrofit. The use of ECC as dampers and joints in aseismic building design is also being considered. The uniquely ductile behavior of ECC makes it an attractive material candidate to handle high stress concentration due to the interaction between steel and concrete in hybrid structures. The objective is to decrease the damage of structures affected by earthquakes. In order to protect life and properties, the response deflection of structures and damage of structural elements should be limited.

### *Cyclic Response of Beam-Column Connection*

On the beam-column connection component level in earthquake resistant design, the following performance are desirable: (i) ductile plastic hinge behavior under high shear stress, (ii) no congestion of transverse reinforcement for confinement and for shear, (iii) maintain concrete integrity under load reversals, and (iv) concrete damage contained within a relatively short hinging zone. These performance are difficult to achieve with ordinary concrete. The sub-assembly of R/C moment resisting frame selected for this test program is

shown schematically in Fig. 7. The test specimen represents two half beams connected to a stub column, in a strong column-weak beam configuration. The beams are simply supported at their ends to represent mid-span inflection points, under lateral loading of a framed structure.

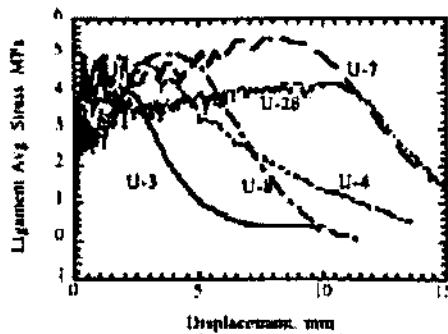


Fig 3: Nominal Stress-Displacement Curves

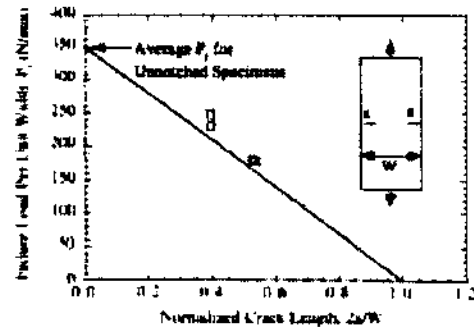


Fig 4: Failure load vs notch depth



Fig. 5: Damage pattern of notched PE-ECC

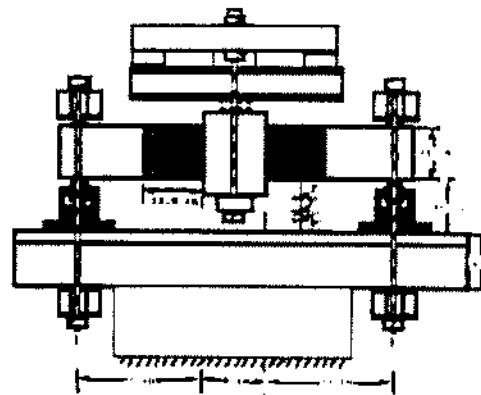


Fig. 7: Schematic of PE-ECC Connection Test

Two specimens, one using plain concrete (PC) for the entire specimen and the other using PE-ECC material in the plastic hinge zone and PC in the rest of the specimen, were tested. Ordinary detailing was used for both specimens to highlight the contribution of the ECC. The loading history used in this testing program consists of simple multiple steps of symmetric cycles of increasing displacement amplitude. The displacement controlled loading sequence, specimen and load details can be found in Li (1997).

The load vs. deflection hysteretic behavior is shown in Fig. 8. For the PC hinge, the displacement ductility factor defined as the ratio of ultimate deflection (corresponding to a failure load that is about 20% lower than the maximum load carrying capacity) to yield deflection of about 4.8. For the ECC hinge, the displacement ductility factor increases to 6.4, with less amount of pinching and a much reduced rate of stiffness degradation. The cracking pattern (Fig. 9) was distinctly different with more cracking taking place in the plastic hinge zone with ECC rather than the zone outside as in the case of the PC control specimen. The damage is mostly in the form of diagonal multiple cracking in perpendicular direction. Unlike the control specimen which fail in a predominantly shear diagonal fracture, the ECC specimen fails by a vertical flexural crack at the interface between ECC plastic hinge zone and the plain concrete at the column face. No spalling was observed in the ECC hinge, whereas the concrete cover mostly disintegrated in the control. The cumulative energy over the load cycles for the two specimens shows that the ECC hinge absorbs about 2.8 times as much energy as the control.

### Shear Wall Panels for Seismic Retrofit

A retrofit method considered consists of a light but ductile shear wall constructed between columns and beams of an existing multistory RC frame building. Under horizontal seismic loads, the frame structure deforms and induces shear loading into the wall. The wall acts as braces in the frame structure, with one diagonal subjected

to compression and the other to tension. It is expected that, if a strong earthquake occurs, the wall undergoes inelastic deformation, namely cracking normal to the tensile diagonal. Energy is dissipated during this inelastic process, which further improves the seismic resistance of the whole structure. After fulfilling its function, the damaged shear wall is removed and replaced by a new one. In order to facilitate the construction and replacement process, the wall is designed as an assembly of prefabricated panels which are jointed together by friction bolts and to the original RC structure by dowel joints (Fig. 10).

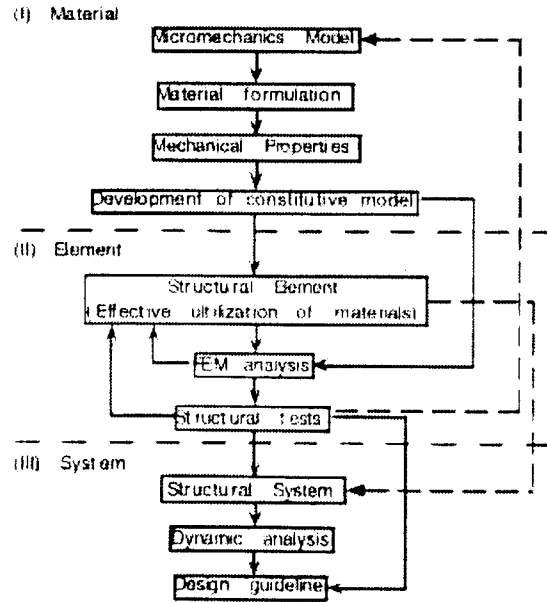


Fig. 6: Framework of Overall Research Program

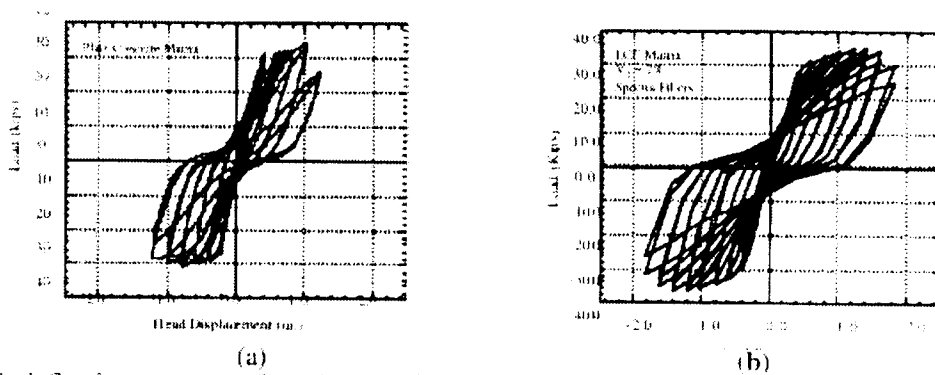


Fig. 8: Load- deflection response of specimen with (a) plain concrete plastic hinge, and (b) ECC plastic hinge

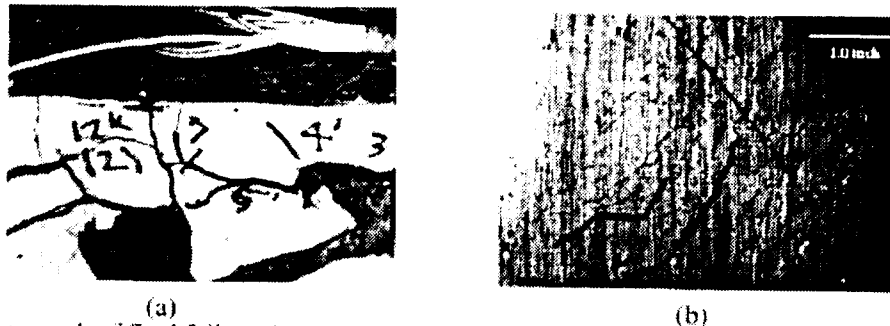


Fig. 9: Photograph of final failure, in the plastic hinge zone of (a) control, and (b) ECC specimens

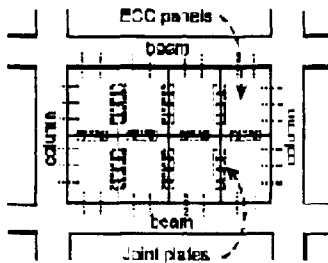


Fig. 10: Seismic Retrofit Shear Wall

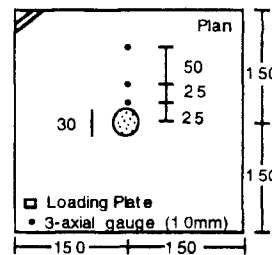


Fig. 11: Indentation Test Configuration

In general, any form of contact between steel and concrete can lead to fracture failure of concrete under severe seismic loads. This has been revealed in anchor failure of the base of building columns in the Kobe earthquake. In addition, contacts between steel and concrete can be expected in hybrid structures such as in steel beam/RC concrete column combination (RCS). The fracture failure is a direct result of (a) high stress concentration due to the contrast between steel and concrete elastic modulus (about one order), and (b) the poor ability of ordinary concrete to dissipate the high stress concentration due to limited tensile strain capacity.

In the present research, focus is placed on the behavior of the ECC under direct steel bolt force, which acts like a punch onto a ECC slab. This action is simulated by an indentation test (Fig. 11). A circular steel plate is pushed into a slab of the specimen which is supported on its underside on a flat surface. Circular indenter size includes 67 mm and 90 mm, besides the 30 mm indicated. Two types of specimens are used, a PVA-ECC and a control specimen with plain mortar. For each specimen type, test is repeated with different load area as a ratio of the slab surface area. Figure 12 shows the load deflection curves for the two specimen types. It is clear that the deformation capacity of the composite is significantly enhanced in the ECC, by as much as an order of magnitude.

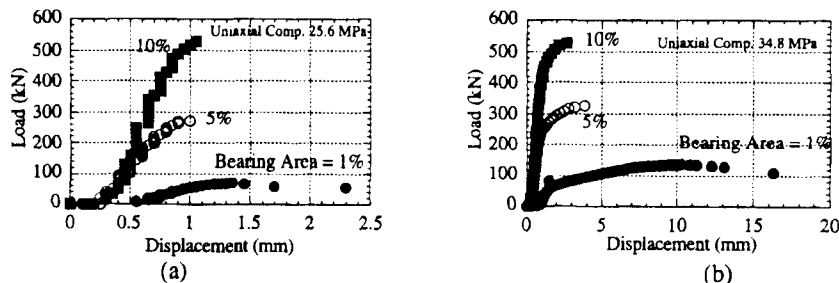


Fig. 12: Load-deflection Curves of Indentation Tests For (a) Mortar, and (b) PVA-ECC

The failed specimens are shown in Fig.13. The mortar reflects the typical response of a brittle material under a flat indenter. Radial fracture leads to complete and catastrophic failure of the specimen. The PVA-ECC specimen shows the flat indenter punching in, without fracture of the specimen. The close up (Fig. 13c) image reveals microcracks, with average width of 24  $\mu\text{m}$  at the edge of the punched depression. The material under the indenter appears to undergo 'plastic yielding', suggesting very high damage tolerance of this brittle matrix composite. This experimental evaluation confirms that the PVA-ECC can be used in shear panels bolt jointed together without fear of fracture failure. It also indicates that shear failure under seismic load is not likely to occur at the joint due to the damage tolerance observed. Numerical simulation (discussed below) seems to confirm this hypothesis. However, direct shear test of the joint should be conducted.

To numerically simulate the mechanical response of a shear panel (Kabele et al, 1997), the material model developed by Kabele (1995) for ECC material was chosen. Among other features, the material model accounts for extensive strain-hardening response under tension for ECC. For this simulation, material parameters were derived from uniaxial tensile and compression tests of PVA-ECC. The simplified geometry of a shear panel and boundary condition adopted is shown in Fig. 14. For the assumed mode of deformation and panel arrangements, the average shear strain  $\gamma_w$  is equal to the relative floor shear displacement  $\gamma_f$ . The panel

dimensions (height  $h = 680$  mm, width  $w = 300$  mm and thickness  $b = 75$ mm) are also chosen to agree with planned experimental setup. In the present analysis, it is assumed that no reinforcing steel bars/mesh are used.

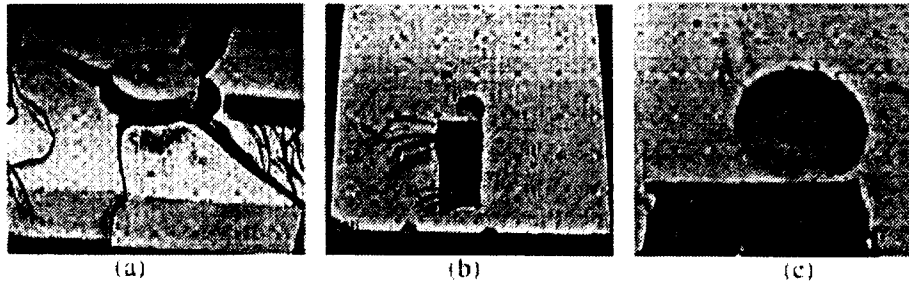


Fig. 13: Failed (a) Mortar (b) PVA-ECC Specimen (c) Close-Up of (b) near indenter

For comparison purpose, a normal concrete is used as the control. Figure 15 shows the computed averaged shear stress versus shear strain behavior. The ECC (Material #1) panel failed at averaged shear load and shear deformation much higher than that of ordinary concrete (Material #2). However, the shear strain at maximum load was limited by the compressive strain capacity, prior to exhausting the tensile strain capacity of the ECC. When the compressive strain capacity was artificially increased (Material #3), the averaged shear load-deformation curve reveals a plastic yield behavior. This analysis shows that for ECC material with extremely high tensile strain capacity and when used without steel reinforcement, the structural capacity may be limited by compression rather than tension failure. If this is confirmed experimentally, this research points to the need to design future ECCs with improved compressive strain capacity.

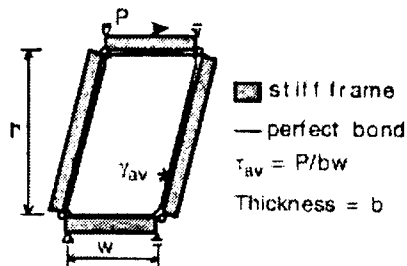


Fig. 14: Simplified Model of Shear Wall Panel

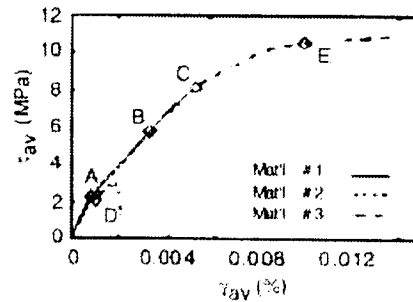


Fig. 15: Computed  $\tau_{av}$ - $\gamma_{av}$  Curves

The development of microcrack pattern throughout the loading process in the ECC panel has been computed. Figure 16 shows that tensile microcracking is initiated at the construction joints. However, these microcracks do not localize, but spreads from the locations of tensile and shear stress concentration. This feature again reconfirms the unique damage tolerance of ECC, discussed in the previous section.

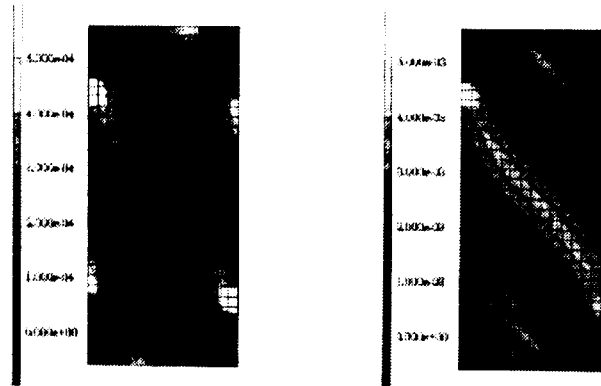


Fig. 16: Maximum Cracking Strain at Load level A (left) and B (right) Indicated in Fig. 15

## CONCLUDING REMARKS AND CONTINUING RESEARCH

This paper surveys some pertinent mechanical properties of ECC designed based on micromechanical principles. A couple of examples in the use of ECC in seismic elements demonstrate the potential of ECC as a high performance ductile cementitious composite suitable for exploitation in structural applications. There are continued needs in research on materials engineering for mechanical property enhancements, including improved strength and compressive strain capacity. Additional material characterization includes mechanical properties under biaxial loading, as well as tension-compression fully reversed cyclic response. Accurate prediction of R/ECC structures will need better knowledge of the interaction between steel reinforcement and ECC. Seismic response analyses of designed structural system with ECC will need to be conducted to study the performance of the structural system and effectiveness of ECC elements. Scaled system tests will be needed prior to full scale demonstration experiments. The continued materials investigations will provide expanded database of material composition and mechanical properties for structural designers. Research at the structural element and system levels will provide feedback to materials engineers for further materials design. The research program has been designed to allow such two-way engagement between materials engineers and structural engineers, for the benefit of ECC material and structural development.

Research in ECC material and structures has involved academics, industrial concerns and government institutions. Such broad spectrum involvement is necessary to bringing the results of these investigations to bear on practical applications. The expected final outputs through the collaborative research between U.S. and Japan will include: (a) Design method for ECC materials; (b) Analytical model and technique for FEM to evaluate the structural element with ECC; and (c) Design guideline for structural systems with ECC elements.

## ACKNOWLEDGMENTS

VCL acknowledges the support of the US National Science Foundation (Grant NSF-G-CMS-9601262) to the Univ. of Michigan, and support of the Univ. of Tokyo while a Visiting Professor there during the start-up cooperative phase in this research project. Special acknowledgments are due to VCL's graduate students, as well as H. Horii, P. Kabele and T. Kanda for their significant contributions to this research. Supports from BRI and Japanese task group on development of ductile cementitious composites are gratefully appreciated.

## REFERENCES

- Kabele, P., *Analytical Modeling and Fracture Analysis of ECC*, PhD Thesis, Univ. of Tokyo, 1995.
- Kabele, P. et al, Use of BMC for Ductile Structural Members, in *Brittle Matrix Composites 5*, 1997, 579-588.
- Kanda, T. and Li, V.C., Effect of Apparent Fiber Strength and Fiber-Matrix Interface Properties on Crack Bridging in Cementitious Composites, Submitted to *ASCE J. of Engineering Mechanics*, Oct., 1997.
- Li, V.C., From Micromechanics to Structural Engineering -- the Design of Cementitious Composites for Civil Engineering Applications, *JSCE J. of Struc. Mechanics and Earthquake Engineering*, 1993, **10**(2), 37-48.
- Li, V.C., Engineered Cementitious Composites -- Tailored Composites Through Micromechanical Modeling, to appear in *Fiber Reinforced Concrete: Present and the Future*, Eds: N. Banthia et al, CSCE, 1997.
- Li, V.C. Damage Tolerance Of Engineered Cementitious Composites, in *Advances in Fracture Research*, Ed. B.L.Karihaloo, Y.W. Mai, M.I. Ripley and R.O. Ritchie, Pub. Pergamon, UK, 1997. 619-630.
- Li, V.C. and Leung, C.K.Y., Steady State and Multiple Cracking of Short Random Fiber Composites, *ASCE J. of Engineering Mechanics*, 1992, **118**(11) 2246 - 2264.
- Li, V.C. et al, Micromechanical Models of Mechanical Response of HPFRCC, *High Performance Fiber Reinforced Cementitious Composites*, Eds. A.E. Naaman and H.W. Reinhardt, 1996, 43-100.
- Li, V.C., Wang, Y. and Backer, S. Effect of Inclining Angle, Bundling, and Surface Treatment on Synthetic Fiber Pull-Out from a Cement Matrix, *J. Composites*, 1990, **21**(2), 132-140.
- Li, V.C., Mishra, D.K., Naaman, A.E., et al. On the Shear Behavior of Engineered Cementitious Composites, *J. of Advanced Cement Based Materials*, 1994, **1**(3) 142-149.
- Maalej, M., Li, V.C., and Hashida, T. Effect of Fiber Rupture on Tensile Properties of Short Fiber Composites, *ASCE J. Engineering Mechanics*, 1995, **121**(8) 903-913.